Vibro-impact Regimes of Adamped Single-mass System with Two Fixed Stops

Ljubiša B. Garić

Assistant Professor
University of Priština in Kosovska Mitrovica
Faculty of Technical Sciences

Nikola D. Nešić

Assistant Professor
University of Priština in Kosovska Mitrovica
Faculty of Technical Sciences

This study examines the periodic vibro-impact (VI) behavior of an externally excited system containing mass, spring, and damper, whose rectilinear motion is bounded by two symmetrical stops. Periodic external coercive force is driving the system, with the period of the oscillator being one or proportional to the period of the external coercive force. The resulting differential equation of motion, coupled with boundary conditions, is solved analytically, and solutions are discussed. The study analyses different types of behavior and includes stability analysis. The research findings outline the determination of the conditions (areas) in which periodic VI modes exist for even and odd values of mode multiplicity. Additionally, the results made it possible to determine the frequency interval for the VI process when the distance between fixed stops is known. By investigating the dynamics of the VI system in this work, results were obtained that allow all possible types of motion to be theoretically defined, as well as results that define areas of motion stability, which allows one to find regimes that may exist in practice. The results obtained in this paper can be applied to improving existing and developing new vibro-impact tools and machines.

Keywords: external excitation force, stability analysis, vibro-impact modes, vibro-impact oscillator, viscous damping force.

1. INTRODUCTION

Vibro-impact (VI) systems with periodic motion have broad applications in industries and engineering bran–ches, such asmechanical and civil engineering, mining, the food industry, etc. Generally, these systems are employed when the intervals between successive im–pacts remain uniform, and the movement is caused by a coercive force,resulting in a range of effects. These impact-induced dynamic phenomena can be either detrimental or advantageous. To maximize efficiency, minimizing the harmful effects (damage) and ampli–fying the beneficial ones is crucial [1-3].

Many authors, such as Wiercigroch et al. [4] and Costa [5] do experimental investigation and practical development of VI systems. VI systems have applica–tionsfor vibratory hammers, hammer drills, and vib–ratory rammers [6] in energy-harvesting devices [7-9], transmission gearboxes [10], seismic protection [11], combustion engines [12], vibration mitigation devices [7], MEMS including AFM [13], etc.

Many authors have studied periodic VI motion. Papers [14-17] describe the behavior of a system con–taining one mass and single-degree-of-freedom (SDOF), which moves on a linear horizontal trajectory. Other authors [18,19] studied periodic dynamical systems with two degrees of freedom, representing a double-impact

oscillator with many engineering applications. Systems in [19] are with variable positions of the stops, i.e., bumpers. Papers [20] and [21] present the results obta–ined by the analysis of the stability of the periodic motion of VI systems with one bumper, which is in [20] fixed and in [21] movable. A similar study but with two stops is presented in [22]. Studies [23] and [24] present the analysis of the periodic motion of oscillatory sys–tems, which collide with one and two stops. Limiters, bumpers, or stops in VI systems can be compliant as well [25].

VI devices can be used to absorbshock impacts, as presented in [26], where the efficiency of these attach–ments is studied in passively absorbing and dissipating substantial amounts of impact energy through the exa–mination of various setups involving primary linear oscillators coupled with VI attachments.

Stefani et al. [11] investigated the potential benefits of utilizing impact occurrences in a two-sided harmo–nically excited VI-isolated SDOF system and control–ling the response.They examined seismic isolated cons–truction, which moves regarding the ground during the earthquake and suggested inserting characteristic VI absorbers.

The paper [27]examines how the attributes of atte–nuation and isolation attachments impact the behavior of SDOF VI systems equipped with two-sided bumpers and gaps through experiments. They examined several different experimental setups, with and without bum–pers, with different bumpers, gaps, acceleration peaks, and amplitude values, and made a parameter analysis.

Brzeski et al. [28] studied the stability of a coupled system of two bodies excited with external harmonic

forces that differ in phase interacting with soft impacts. They proposed a methodology to narrow down the possible solutions by carefully selecting the gap and phase difference of the periodic excitation force.

Mélot et al. [29] studied the VI behavior of big gear systems. Firstly, they made model reductions followed by obtaining periodic solutions for the system by jointly using the harmonic balance method and path-following techniques such as arc-length numerical continuation [30, 31]. The initiation and cessation of VI reactions are analyzed by computing grazing bifurcations.

Papers [32, 33] investigated the VI behavior of a harm\onically excited oscillator with two degrees of freedom. They studied the variety and progression of periodic impact motions, focusing on transitions to non-periodic and chaotic motions, along with various bifur–cation types and shifts between them. The impact velocities and existence areas of various types of peri–odic motions of the VI system are studied, focusing on the influence of dynamic parameters within the sampled parameter ranges. Papers [32, 33] differ only in physical models, but the same analysis and methodology are applied.

Liu and Chavez [34] focused on stabilizing a VI capsule system under periodic excitation load. The capsule can move both forward and backward along a straight path. Their primary goal was to regulate this motion direction. They showed that the system's motion can be controlled by appropriately adjusting its initial conditions without any modification to the system parameters.

As in other areas of mathematics, physics, and engineering sciences, in the area of VI systems, the research trend is to use numerical methods [35, 36]. Those methods may lead to the wrong results if the initial conditions are wrongly assumed, and for a certain set of parameters, the solutions diverge. It is also difficult to determine the areas where the solutions converge to the exact solution. That is why analytical solutions like those in this work are advantageous. Certainly, numerical methods must be used for significantlymore complex models, but this work can be used to make a good assumption of the initial solution so that a more complex problem can be solved.

Scientific publications [1,37,38] include the results obtained by analyzing VI systems dynamics using appropriate mathematical models. The analysis of the model motion defines different modes of motion and investigates the conditions for the existence of these modes. In publication [1], Babicki investigates the peri–odic motion of VI systems with a known period of oscillation and presents the results that define periodic motion's stability.

The research of this paper follows this guideline. Besides that, similar to [1, 13],in this paper, the period of oscillation is equal or proportional to the period of external excitation force. Compared to paper [1], here is a presented phase plane with two different damping decrements. Additionally, VI analysis in [1] includes only odd numbers for a multiplicity of the mode, while more general analysis is presented here, including both even and odd numbers for the multiplicity of the mode, i.e. $l = 1, 2, 3, 4, 5, ...$

Based on the analysis of VI systems, different mac–hines can be constructed where the working part performs periodic [1,39] and nonperiodic vibration impacts [39,40], depending on the nature of the tech–nological process. VI systems have vast applications in engineering, including construction machines, casting machines, transport machines, etc.
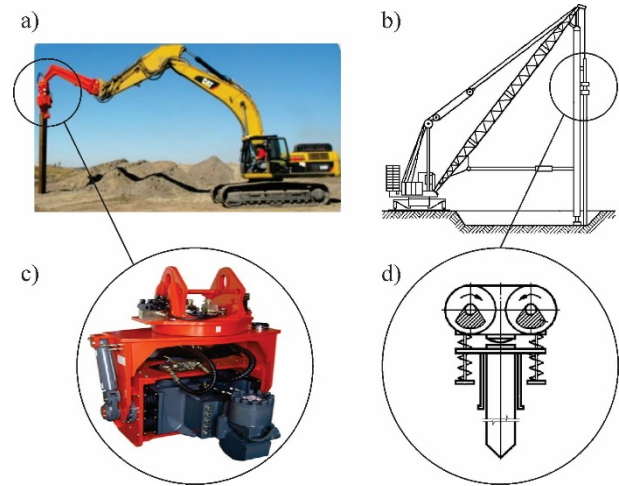

Figure 1. Vibratory Hammer:a) Driving sheet pile 400mm x 6m[41], b) Shema of machine driving sheet pile/beam/pipes [6], c) Sheet pile driver [41], d) Sheet pile driver - Shema [6].
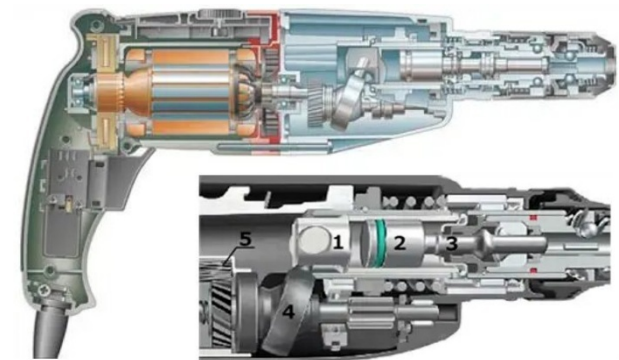

Figure 2. Hammer drill machine [42]: 1) cylinder, 2) piston, 3) striker, 4) swinging bearing, 5) engine gear
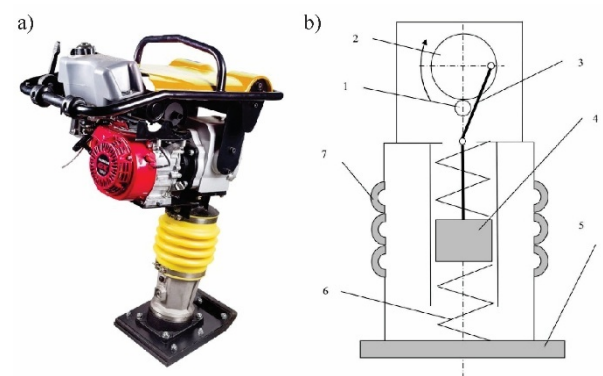

Figure 3. Vibratory rammer[43]: a) STEM Techno STR81/STR82, b) Scheme of STEM Techno STR81/STR82:1) gear, 2) wheel, 3) piston rod, 4) piston, 5) tamping plate, 6) spring, 7) shock absorber.

Several machines can be constructed using a mathe–matical model of a horizontal or vertical single-mass VI system with two stationary stops, such as a vibro hammer (Fig. 1), hammer drill machine (Fig. 2), vibratory rammer (Fig. 3), etc. Vibro hammers, which

are used to drive rods, pipes, and other elements into the ground, represent a large part of the area of VI systems. Figure 1 shows the appearance and scheme of the vibratory hammer. A vibratory rammer (Fig 3.) is a machine with periodic movement, which acts on the surface of the soil to smooth out unevenness, as well as to increase the density of the soil before laying asphalt, concrete, etc.

The topic of this research is the analysis of a horizontal straight-line motion of a single-mass VI system with two symmetrical stops placed on both sides of the oscillator when a periodic VI mode is realized in the system. The motion analysis of the VI system is done using a mathematical model shown in Figure 4. The main result is the determination of the conditions (areas) in which periodic VI modes exist. The results of the research enable movement stability for the VI system. All graphical results are presented by using Mathcad 14 software.

2. MATHEMATICAL MODEL AND EQUATION OF MOTION

Figure 4 shows a mathematical model of a horizontal rectilinear motion of a single-mass VI system with two symmetrical stopsplaced on both sides of the oscillator, which is exposed to the force $F_e = c_y \cdot y$ of spring with stiffness c_y, viscous damping force $F_w = b_y \cdot \dot{y}$ with proportionality coefficient b_y, and external periodic excitation force:

$$F(t) = \sum_{i=1}^{k} F_i \cdot \cos\left(i \cdot \Omega \cdot t + \varphi_i\right) \quad (1)$$

One fixed stop is placed at a distance $y = \Delta$ to the right of the equilibrium position, i.e. point O. Another fixed stop is at a distance $y = -\Delta$ to the left of the equilibrium position, i.e. point O. The mass of the oscillator impacts alternately to the right and left stops, so one period of oscillator movement $T = 2\pi / \Omega$ consists of two equal half-periods of movement $T_1 = E_2 = \pi/\Omega$. The first half-period T_1 includes the time of oscillator movement from the impact to the right stop up to the impact to the left stop.

In addition, the second half-period T_2 includes the time of traveling of the VI oscillator from the impact into the left stop up to the impact into the right stop. Since all movement intervals are identical, it is suffi–cient to examine just one interval of the oscillator's motion between two consecutive impacts.

The motion of the dynamical system between two successive impactspresented in Figure 4 can be described with the following differential equation:

$$m \cdot \ddot{y} + b_y \cdot \dot{y} + c_y \cdot y = F(t) = \sum_{i=1}^{k} F_i \cdot \cos\left(i \cdot \Omega \cdot t + \varphi_i\right). \quad (2)$$

The mass m of the oscillator is assumed to be constant. Eq. (2) can be written in extended form as:

$$m \cdot \ddot{y} + b_y \cdot \dot{y} + c_y \cdot y = F_1 \cos\left(\Omega \cdot t + \varphi_1\right) + \\ + F_2 \cos\left(2 \cdot \Omega \cdot t + \varphi_2\right) + ... + F_k \cos\left(k \cdot \Omega \cdot t + \varphi_k\right). \quad (3)$$
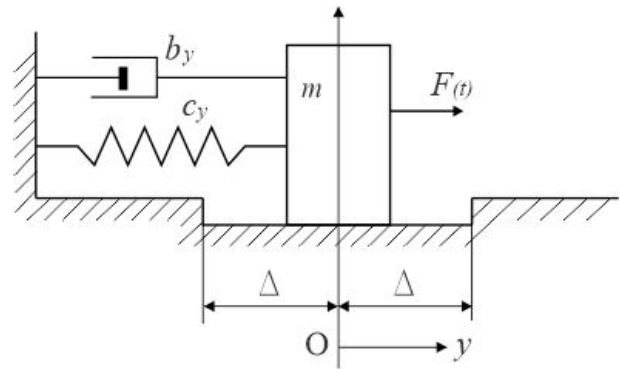

Figure 4. Mathematical model of a VI oscillator with two stops

If both sides of equation (3) are divided by m, the following equation can be obtained:

$$\ddot{y} + \frac{b_y}{m} \dot{y} + \frac{c_y}{m} y = \frac{F_1}{m} \cos\left(\Omega \cdot t + \varphi_1\right) + \\ + \frac{F_2}{m} \cos\left(2 \cdot \Omega \cdot t + \varphi_2\right) + ... + \frac{F_k}{m} \cos\left(k \cdot \Omega \cdot t + \varphi_k\right). \quad (4)$$

If it is taken into consideration tha t $n = \dfrac{b_y}{2m}$ is the damping constant: $\omega_y^2 = \dfrac{c_y}{m}$ is the natural circular fre–quency of the linear oscillator without stops, Ω is the circular frequency of the excitation force, φ is the initial phase of the excitation forces $P_1 = \dfrac{F_1}{m}$, $P_2 = \dfrac{F_2}{m}$, ..., $P_k = \dfrac{F_k}{m}$, the following equation is obtained:

$$\ddot{y} + 2n \cdot \dot{y} + \omega_y^2 \cdot y = P_1 \cos\left(\Omega \cdot t + \varphi_1\right) + \\ + P_2 \cos\left(2 \cdot \Omega \cdot t + \varphi_2\right) + ... + P_\kappa \cos\left(\kappa \cdot \Omega \cdot t + \varphi_\kappa\right). \quad (5)$$

According to the theory of differential equations, the general solution of (5) consists of the sum of the solu–tions of the homogeneous part of the equation y_h, as well as the particular solutions y_{1p}, y_{2p}, ..., y_{kp}, where the solution of the homogeneous part is:

$$y_h = e^{-n \cdot t} \left(B_1 \cos\left(\sqrt{\omega_y^2 - n^2} \cdot t\right) + B_2 \sin\left(\sqrt{\omega_y^2 - n^2} \cdot t\right) \right) \quad (6)$$

where the expression $\Omega_1 = \sqrt{\omega_y^2 - n^2}$ represents the damped circular frequency.

The unknown constants B_1 and B_2 in equation (6) areobtained by applying the conditions of periodic motion which are defined by expressions (23), (24), (25) and (26) in the following part of this paper.

If $B_1 = D\cos(\delta)$ and $B_2 = -D\sin(\delta)$ are assumed, equation (6) will take the following form:

$$y_h = e^{-n \cdot t} \left(D\cos(\delta) \cdot \cos\left(\sqrt{\omega_y^2 - n^2} \cdot t\right) - D\sin(\delta) \cdot \sin\left(\sqrt{\omega_y^2 - n^2} \cdot t\right) \right) \quad (7)$$

If the equation $\cos(\alpha + \beta) = \cos\alpha\cos\beta - \sin\alpha\sin\beta$ is used, the following is obtained:

$$y_h = D \cdot e^{-n \cdot t} \cos\left(\sqrt{\omega_y^2 - n^2} \cdot t + \delta\right) \qquad (8)$$

where $D = \sqrt{B_1^2 + B_2^2}$ and $tg(\delta) = -\dfrac{B_2}{B_1}$.

Further, as will be shown later in this paper, the particular solutions y_{1p}, y_{2p}, ..., y_{kp} of the differential equation (5) are determined.

At the beginning, only the first term on the right hand side of (5) is taken into consideration, leading to

$$\ddot{y} + 2n \cdot \dot{y} + \omega_y^2 \cdot y = P_1 \cos(\Omega \cdot t + \varphi_1) \qquad (9)$$

Then, the particular solution is assumed to be:

$$y_{1p} = M_1 \cos(\Omega \cdot t + \varphi_1) + N_1 \sin(\Omega \cdot t + \varphi_1) \qquad (10)$$

When the first and second derivatives of equation (10) are determined and substituted into (9), the follo–wing equations are obtained:

$$M_1 = \frac{P_1\left(\omega_y^2 - \Omega^2\right)}{4n^2 \cdot \Omega^2 + \left(\omega_y^2 - \Omega^2\right)^2},$$

$$N_1 = \frac{P_1 \cdot 2n \cdot \Omega}{4n^2 \cdot \Omega^2 + \left(\omega_y^2 - \Omega^2\right)^2}. \qquad (11)$$

After introducing $p = \dfrac{\Omega}{\omega_y}$ as a dimensionless frequ–ency and $\Delta_y = \dfrac{\pi \cdot b_y}{m \cdot \omega_y} = \dfrac{2\pi n}{\omega_y}$ as a damping decrement,

it is obtained

$$M_1 = \frac{Y_1\left(1 - p^2\right)}{\left(\dfrac{\Delta_y}{\pi}\right)^2 p^2 + \left(1 - p^2\right)^2},$$

$$N_1 = \frac{Y_1 \dfrac{\Delta_x}{\pi} p}{\left(\dfrac{\Delta_y}{\pi}\right)^2 p^2 + \left(1 - p^2\right)^2}, \qquad (12)$$

Where $Y_i = \dfrac{F_i}{c_y}$ is the static elongation of the spring

under the action of force F_i, where $i = 1, \ldots k$.

I f $K_1(p) = \left(\dfrac{\Delta_y}{\pi}\right)^2 p^2 + \left(1 - p^2\right)^2$ is adopted, the

particular solution (10) has the form:

$$y_{1p} = \frac{Y_1\left(1 - p^2\right)}{K_1(p)} \cos(\Omega \cdot t + \varphi_1) +$$

$$+ \frac{Y_1 \dfrac{\Delta_x}{\pi} p}{K_1(p)} \sin(\Omega \cdot t + \varphi_1) \qquad (13)$$

The general solution for the differential equation (9) has the form $y_1 = y_h + y_{1p}$, i.e.

$$y_1 = D \cdot e^{-n \cdot t} \cos\left(\sqrt{\omega_y^2 - n^2} \cdot t + \delta\right) +$$

$$+ \frac{Y_1\left(1 - p^2\right)}{K_1(p)} \cos(\Omega \cdot t + \varphi_1) + \frac{Y_1 \dfrac{\Delta_x}{\pi} p}{K_1(p)} \sin(\Omega \cdot t + \varphi_1) \qquad (14)$$

When only the last term on the right side of equation (5) is taken into account, the particular solution is determined as:

$$\ddot{y} + 2n \cdot \dot{y} + \omega_y^2 \cdot y = P_k \cos(k \cdot \Omega \cdot t + \varphi_k) \qquad (15)$$

The particular solution is assumed to be of the form:

$$y_{kp} = M_k \cos(k \cdot \Omega \cdot t + \varphi_k) + N_k \sin(k \cdot \Omega \cdot t + \varphi_k). \qquad (16)$$

When the first and second derivatives of equation (16) are determined and substituted into (15), the following equations are obtained:

$$M_k = \frac{P_k\left(\omega_y^2 - k^2 \cdot \Omega^2\right)}{4n^2 \cdot k^2 \cdot \Omega^2 + \left(\omega_y^2 - k^2 \cdot \Omega^2\right)^2}$$

$$N_k = \frac{P_k \cdot 2n \cdot \Omega \cdot k}{4n^2 \cdot k^2 \cdot \Omega^2 + \left(\omega_y^2 - k^2 \cdot \Omega^2\right)^2} \qquad (17)$$

After simple mathematical transformations of equa–tions (17), following is obtained:

$$M_k = \frac{Y_k\left(1 - k^2 \cdot p^2\right)}{\left(\dfrac{\Delta_y}{\pi}\right)^2 k^2 \cdot p^2 + \left(1 - k^2 \cdot p^2\right)^2}$$

$$N_k = \frac{Y_k \dfrac{\Delta_x}{\pi} p \cdot k}{\left(\dfrac{\Delta_y}{\pi}\right)^2 k^2 \cdot p^2 + \left(1 - k^2 \cdot p^2\right)^2} \qquad (18)$$

If $K_k(p) = \left(\dfrac{\Delta_y}{\pi}\right)^2 k^2 \cdot p^2 + \left(1 - k^2 \cdot p^2\right)^2$ is adop–

ted, the particular solution (16) has the form:

$$y_{kp} = \frac{Y_k\left(1 - k^2 \cdot p^2\right)}{K_k(p)} \cos(k \cdot \Omega \cdot t + \varphi_k) +$$

$$+ \frac{Y_k \dfrac{\Delta_y}{\pi} p \cdot k}{K_k(p)} \sin(k \cdot \Omega \cdot t + \varphi_k) \qquad (19)$$

The general solution for the differential equation (15) has the for $y_k = y_h + y_{kp}$, i.e.

$$y_k = D \cdot e^{-n \cdot t} \cos\left(\sqrt{\omega_y^2 - n^2} \cdot t + \delta\right) +$$

$$+ \frac{Y_k\left(1 - k^2 \cdot p^2\right)}{K_k(p)} \cos(k \cdot \Omega \cdot t + \varphi_k) +$$

$$+ \frac{Y_k \dfrac{\Delta_y}{\pi} p \cdot k}{K_k(p)} \sin(k \cdot \Omega \cdot t + \varphi_k) \qquad (20)$$

Finally, the particular solutions of the differential equation (5) are determined for the case when there are k addends on the right side. In that case k particular solutions are obtained too. The general solution of (5) is

$$y = D \cdot e^{-n \cdot t} \cos\left(\sqrt{\omega_y^2 - n^2} \cdot t + \delta\right) +$$

$$+ \sum_{i=1}^{k} \frac{Y_i \left(1 - i^2 \cdot p^2\right)}{K_i(p)} \cos\left(i \cdot \Omega \cdot t + \varphi_i\right) + \quad (21)$$

$$+ \sum_{i=1}^{k} \frac{Y_i \frac{\Delta_x}{\pi} p \cdot i}{K_i(p)} \sin\left(i \cdot \Omega \cdot t + \varphi_i\right).$$

In analyzing the movement of the VI system, observing a single interval of the oscillator's motion between two successive impacts is sufficient. Each impact is part of a sequence of successive impacts, and VI processes with an endless series of impacts are referred to as infinite impacts [1,3]. This paper inves–tigates the periodic motion of a VI system, assuming that the oscillation period is equal to or proportional to the period of the excitation force. A key feature of VI systems is the potential for various modes of motion. Therefore, research on these systems should define all possible motion types and analyze their stability. This approach aims to identify and isolate movement modes that could realistically occur in practice.

The effect of an impact is accounted for using the restitution coefficient at each impact $0 \le R \le 1$. For $R = 0$ impact is plastic, while for $R = 1$ it is absolutely elastic. In this example, it is assumed that the coeffi–cients of restitution on impact are the same for both stops. Assuming the oscillator's velocity is $\dot{y}_-$ just be–fore an impact and $\dot{y}_+$ just after the impact, these two velocities are related by the following equation:

$$\dot{y}_+ = -R \cdot \dot{y}_- . \quad (22)$$

3. BOUNDARY CONDITIONS FOR THE EXISTENCE OF PERIODIC VI MODES

The period of movement of the VI oscillator $T = 2\pi/\Omega$ shown in Figure 4 consists of two equal half-periods of movement $T_1 = T_2 = \pi/\Omega$. Impacts occur alternately in the right and left stops at constant intervals that are proportional to the half-period of the excitation force $\pi \cdot l/\Omega$, where l is the multiplicity of the mode.

For $l = 1$, the oscillator crosses the path from the right to the left stop for one half-period of change in the excitation force $F(t)$. For $l = 2$ the oscillator travels from the right to the left stop for two half-periods of change in the excitation force $F(t)$. For $l = 3$, the oscillator crosses the path from the right to the left stop for three half-periods of change in the excitation force $F(t)$, and so on.

The boundary conditions for the first half-period T_1 of the oscillator movement are:

$$t = 0 , \; y(0) = \Delta , \quad \dot{y}(0) = \dot{y}_+ = -R \cdot \dot{y}_- . \quad (23)$$

$$T_1 = \frac{\pi \cdot l}{\Omega} , \; y(T_1) = -\Delta , \quad \dot{y}(T_1) = -\dot{y}_- . \quad (24)$$

where Eq. (23) denotes the beginning of the cycle, i.e. the moment after impact to the right stop, while Eq.(24) presents the end of the cycle, i.e., the moment before the next impact to the left stop.

For the second half-period T_2, the following boundary conditions are introduced:

$$t = 0 , \; y(0) = -\Delta , \quad \dot{y}(0) = \dot{y}_+ = R \cdot \dot{y}_- \quad (25)$$

$$T_2 = \frac{\pi \cdot l}{\Omega} , \; y(T_2) = \Delta , \; \dot{y}(T_2) = \dot{y}_- . \quad (26)$$

where Eq. (25) describe the beginning of the cycle, i.e the moment after impact to the left stop, while Eq.(26) represents the end of the cycle, i.e, the moment before the next impact to the right stop.

In the analysis of the oscillator movement, the first half-period is observed. This period begins after the impact to the right stop and lasts until the next impact to the left stop. The boundary conditions (23) and (24) are used in the calculation. The equation describing the motion of the oscillator in the first half-period has the form (14).

If $\quad A\cos(\delta) = \dfrac{Y_1\left(1 - p^2\right)}{K_1(p)} \quad$ and $\quad A\sin(\delta) = -\dfrac{Y_1 \frac{\Delta_y}{\pi} p}{K_1(p)}$

are assumed, (14) is expressed as follows:

$$y = D \cdot e^{-n \cdot t} \cos\left(\sqrt{\omega_y^2 - n^2} \cdot t + \delta\right) + A\cos\left(\Omega \cdot t + \varphi_1 + \delta\right) \quad (27)$$

where

$$A = \sqrt{\left(\frac{Y_1\left(1 - p^2\right)}{K_1(p)}\right)^2 + \left(-\frac{Y_1 \frac{\Delta_x}{\pi} p}{K_1(p)}\right)^2} , \quad tg(\delta) = -\frac{\frac{\Delta_y}{\pi} p}{\left(1 - p^2\right)} .$$

The equation for A represents the amplitude of excitation oscillations that are caused by the external excitation force $F_1(t) = F_1 \cos\left(\Omega \cdot t + \varphi_1\right)$.

If equation (6) is used for solving the homogeneous part of equation (5) and if $\psi = \varphi_1 + \delta$ is assumed, then (27) is expressed as follows:

$$y = e^{-n \cdot t}\left(B_1 \cos\left(\sqrt{\omega_y^2 - n^2} \cdot t\right) + B_2 \sin\left(\sqrt{\omega_y^2 - n^2} \cdot t\right)\right) + A\cos\left(\Omega \cdot t + \psi\right) \quad (28)$$

If small values of the viscous damping coefficient are taken into consideration (i.e. $n << \omega_y$), then $\Omega_1 = \sqrt{\omega_y^2 - n^2} \approx \omega_y$ (i.e. $\Omega_1 = \omega_y$).

When this is taken into account, equation (28) has the following form:

$$y = e^{-n \cdot t}\left(B_1 \cos\left(\omega_y t\right) + B_2 \sin\left(\omega_y t\right)\right) + A\cos\left(\Omega \cdot t + \psi\right). \quad (29)$$

After taking the first time derivative of (29), velocity is obtained as

$$\dot{y} = -n \cdot e^{-n \cdot t} \left(B_1 \cos\left(\omega_y t\right) + B_2 \sin\left(\omega_y t\right) \right) +$$
$$+ e^{-n \cdot t} \left(-B_1 \, \omega_y \sin\left(\omega_y t\right) + B_2 \, \omega_y \cos\left(\omega_y t\right) \right) - \quad (30)$$
$$- A \cdot \Omega \cdot \sin\left(\Omega \cdot t + \psi\right).$$

The boundary conditions for the first half-period of motion (23) and (24) are used to determine the constants B_1 and B_2. The procedure for determining the constants B_1 and B_2 is presented below.

After substituting the boundary conditions (23) into equations (29) and (30), the following is obtained:

$$\Delta = B_1 + A\cos\left(\psi\right)$$
$$-R \cdot \dot{y}_- = -n \cdot B_1 + \omega_y \cdot B_2 - A \cdot \Omega \cdot \sin\left(\psi\right). \quad (31)$$

When the second equation in (31) is divided by ω_y, the following is obtained:

$$\frac{-R \cdot \dot{y}_-}{\omega_y} = -\frac{\Delta_y}{2\pi} B_1 + B_2 - A \cdot p \cdot \sin\left(\psi\right) \quad (32)$$

After substituting the boundary conditions (24) into (29) and (30), the following is obtained:

$$-\Delta = e^{-n \cdot t} \left(B_1 \cos\left(\omega_y \frac{\pi \cdot l}{\Omega}\right) + B_2 \sin\left(\omega_y \frac{\pi \cdot l}{\Omega}\right) \right) +$$
$$+ A\cos\left(\pi \cdot l + \psi\right),$$
$$-\dot{y}_- = -n \cdot e^{-n\frac{\pi \cdot l}{\Omega}} \left(B_1 \cos\left(\omega_y \frac{\pi \cdot l}{\Omega}\right) + B_2 \sin\left(\omega_y \frac{\pi \cdot l}{\Omega}\right) \right) + \quad (33)$$
$$+ \omega_y \cdot e^{-n\frac{\pi \cdot l}{\Omega}} \left(-B_1 \sin\left(\omega_y \frac{\pi \cdot l}{\Omega}\right) + B_2 \cos\left(\omega_y \frac{\pi \cdot l}{\Omega}\right) \right) -$$
$$- A \cdot \Omega \cdot \sin\left(\pi \cdot l + \psi\right).$$

When the second equation of equations (33) is divided by ω_y, the following is obtained:

$$\frac{-\dot{y}_-}{\omega_y} = -\frac{\Delta_y}{2\pi} \cdot e^{-\frac{\Delta_y l}{2p}} \left(B_1 \cos\left(\frac{\pi \cdot l}{p}\right) + B_2 \sin\left(\frac{\pi \cdot l}{p}\right) \right) +$$
$$+ e^{-\frac{\Delta_y l}{2p}} \left(-B_1 \sin\left(\frac{\pi \cdot l}{p}\right) + B_2 \cos\left(\frac{\pi \cdot l}{p}\right) \right) - \quad (34)$$
$$- A \cdot p \cdot \sin\left(\pi \cdot l + \psi\right)$$

In equation (34), the trigonometric function $\sin\left(\pi \cdot l + \psi\right)$ should be tested as follows:

- when $l = 1 \Rightarrow \sin\left(\pi \cdot 1 + \psi\right) = -\sin\left(\psi\right)$,
- when $l = 2 \Rightarrow \sin\left(\pi \cdot 2 + \psi\right) = \sin\left(\psi\right)$,
- when $l = 3 \Rightarrow \sin\left(\pi \cdot 3 + \psi\right) = -\sin\left(\psi\right)$,
- when $l = 4 \Rightarrow \sin\left(\pi \cdot 4 + \psi\right) = \sin\left(\psi\right)$, etc.

Thus, when l is odd, the value $-\sin\left(\psi\right)$ is obtained, and when l is even, the value $\sin\left(\psi\right)$ is obtained.

When l is odd, i.e. $l = 1,3,\ldots$, equation (34) has the following form:

$$\frac{-\dot{y}_-}{\omega_y} = -\frac{\Delta_y}{2\pi} \cdot e^{-\frac{\Delta_y l}{2p}} \left(B_1 \cos\left(\frac{\pi \cdot l}{p}\right) + B_2 \sin\left(\frac{\pi \cdot l}{p}\right) \right) +$$
$$+ e^{-\frac{\Delta_y l}{2p}} \left(-B_1 \sin\left(\frac{\pi \cdot l}{p}\right) + B_2 \cos\left(\frac{\pi \cdot l}{p}\right) \right) + A \cdot p \cdot \sin\left(\psi\right) \quad (35)$$

When l is even, i.e. $l = 2,4,\ldots$, equation (34) has the following form:

$$\frac{-\dot{y}_-}{\omega_y} = -\frac{\Delta_y}{2\pi} \cdot e^{-\frac{\Delta_y l}{2p}} \left(B_1 \cos\left(\frac{\pi \cdot l}{p}\right) + B_2 \sin\left(\frac{\pi \cdot l}{p}\right) \right) +$$
$$+ e^{-\frac{\Delta_y l}{2p}} \left(-B_1 \sin\left(\frac{\pi \cdot l}{p}\right) + B_2 \cos\left(\frac{\pi \cdot l}{p}\right) \right) - A \cdot p \cdot \sin\left(\psi\right). \quad (36)$$

The first equation in (33) can be written in the following form:

$$-\Delta = e^{-\frac{\Delta_y l}{2p}} \left(B_1 \cos\left(\frac{\pi \cdot l}{p}\right) + B_2 \sin\left(\frac{\pi \cdot l}{p}\right) \right) +$$
$$+ A\cos\left(\pi \cdot l + \psi\right). \quad (37)$$

In equation (37), the trigonometric function $\cos\left(\pi \cdot l + \psi\right)$ should be tested as follows:

when $l = 1 \Rightarrow \cos\left(\pi \cdot 1 + \psi\right) = -\cos\left(\psi\right)$,

when $l = 2 \Rightarrow \cos\left(\pi \cdot 2 + \psi\right) = \cos\left(\psi\right)$,

when $l = 3 \Rightarrow \cos\left(\pi \cdot 3 + \psi\right) = -\cos\left(\psi\right)$,

when $l = 4 \Rightarrow \cos\left(\pi \cdot 4 + \psi\right) = \cos\left(\psi\right)$, etc.

Thus, when l is odd, the value $-\cos\left(\psi\right)$ is obtained, and when l is even, the value $\cos\left(\psi\right)$ is obtained.

When l is odd, i.e. $l = 1,3,\ldots$, equation (37) has the following form:

$$-\Delta = e^{-\frac{\Delta_y l}{2p}} \left(B_1 \cos\left(\frac{\pi \cdot l}{p}\right) + B_2 \sin\left(\frac{\pi \cdot l}{p}\right) \right) - A\cos\left(\psi\right) \quad (38)$$

When l even, i.e. $l = 2,4,\ldots$, equation (37) has the following form:

$$-\Delta = e^{-\frac{\Delta_y l}{2p}} \left(B_1 \cos\left(\frac{\pi \cdot l}{p}\right) + B_2 \sin\left(\frac{\pi \cdot l}{p}\right) \right) + A\cos\left(\psi\right) \quad (39)$$

3.1 Regions for the existence of periodic VI regimes when l is an odd number

For the case when $l = 1,3,5,7\ldots$ equations (31), (32), (35), (38) are combined into one system:

$$\Delta = B_1 + A\cos\left(\psi\right),$$

$$\frac{-R \cdot \dot{y}_-}{\omega_y} = -\frac{\Delta_y}{2\pi} B_1 + B_2 - A \cdot p \cdot \sin\left(\psi\right),$$

$$-\Delta = e^{-\frac{\Delta_y l}{2p}}\left(B_1 \cos\left(\frac{\pi \cdot l}{p}\right) + B_2 \sin\left(\frac{\pi \cdot l}{p}\right)\right) - A\cos(\psi) \quad (40)$$

$$\frac{-\dot{y}_-}{\omega_y} = -\frac{\Delta_y}{2\pi} \cdot e^{-\frac{\Delta_y l}{2p}}\left(B_1 \cos\left(\frac{\pi \cdot l}{p}\right) + B_2 \sin\left(\frac{\pi \cdot l}{p}\right)\right) +$$

$$+ e^{-\frac{\Delta_y l}{2p}}\left(-B_1 \sin\left(\frac{\pi \cdot l}{p}\right) + B_2 \cos\left(\frac{\pi \cdot l}{p}\right)\right) + A \cdot p \cdot \sin(\psi)$$

From the system of equations (40) the following is obtained:

$$B_1 = \Delta - A\cos(\psi), \ B_2 = -B_1 \cdot d_1,$$

$$d_1 = \frac{e^{\frac{\Delta_y l}{2p}} + \cos\left(\frac{\pi \cdot l}{p}\right)}{\sin\left(\frac{\pi \cdot l}{p}\right)}, \quad (41)$$

$$D_1 = \frac{(R+1)\sin\left(\frac{\pi \cdot l}{p}\right)}{2\cos\left(\frac{\pi \cdot l}{p}\right) + e^{\frac{\Delta_y l}{2p}} + e^{-\frac{\Delta_y l}{2p}}},$$

$$S_1 = \frac{1}{p}\left(\frac{R}{D_1} - \frac{e^{\frac{\Delta_y l}{2p}} + \cos\left(\frac{\pi \cdot l}{p}\right) + \frac{\Delta_y}{2\pi}\sin\left(\frac{\pi \cdot l}{p}\right)}{\sin\left(\frac{\pi \cdot l}{p}\right)}\right) \quad (42)$$

$$\sin(\psi) = \frac{\dot{y}_- \cdot D_1}{\omega_y \cdot A} \cdot S_1, \ \cos(\psi) = \frac{\Delta}{A}\left(1 - \frac{\dot{y}_- \cdot D_1}{\omega_y \cdot \Delta}\right) \quad (43)$$

After several transformations in (43), the velocity becomes:

$$\dot{y}_- = \frac{1 \pm \sqrt{1 - \left(S_1^2 + 1\right)\cdot\left(1 - \frac{A^2}{\Delta^2}\right)}}{D_1 \cdot \left(S_1^2 + 1\right)} \cdot \omega_y \cdot \Delta \quad (44)$$

The analysis of equation (44) identifies the regions where VI modes exist. To begin, it is necessary to determine the range of real velocity $\dot{y}_-$ values, which can be obtained by assuming that the expression under the square root in equation (44) is greater than zero, i.e. $1 - \left(S_1^2 + 1\right)\cdot\left(1 - A^2/\Delta^2\right) \geq 0$. Based on this, the first condition that defines the region containing real velocity $\dot{y}_-$ values is expressed as follows:

$$\frac{|\Delta|}{A} \leq \sqrt{1 + \frac{1}{S_1^2}} \quad (45)$$

For the case when $0 < \Delta < A$, VI modes can exist in the region where the stop is positioned within the

bounds of the oscillation amplitude of the VI oscillator. For $\Delta > A$ the oscillation happens without any impact.

When the VI system moves, the oscillation path of the oscillator does not exceed the fixed stops:

$$-\Delta \leq x(t) \leq \Delta \quad \text{or} \quad |x(t)| \leq \Delta \quad (46)$$

Based on the previous condition, it is not possible to precisely find the regions where the VI modes exist.

To find the regions where VI modes exist, a second condition is introduced: the velocity must be greater than zero, i.e.

$$\dot{y}_- > 0 \quad (47)$$

The regions of existence of the VI are determined from the equation for velocity (44), by examining when condition (47) is satisfied. If the term under the square root in equation (44) is assumed to be positive (condition (45)), the velocity will have two distinct values: one positive and one negative. To determine when the velocity is positive, the sign of D_1 is analyzed first. If both the numerator and denominator of D_1 have the same sign, D_1 will always be positive.

The numerator and denominator are analyzed separately as shown below.

Firstly, is analysed numerator in the equation for D_1 where the value $(R + 1)$ is always positive. Sine function in the numerator is positive for $p > l$, and negative when $p < l$, that means that the numerator is positive for $p > l$ and negative when $p < l$.

The graph of the denominator of the expression D_1, given by function:

$$f1(p) = 2\cos\left(\frac{\pi \cdot l}{p}\right) + e^{\frac{\Delta_y l}{2p}} + e^{-\frac{\Delta_y l}{2p}},$$

is shown in Figure 5. The graph was constructed for $l = 1$ and $\Delta_y = 0.2\pi$. The graph is positive for the whole interval $p \in [0,\infty]$, and shows that the denomi–nator is positive. At the end, it can be concluded that the sign for D_1 is determined only by the sinusoidal function of the numerator.
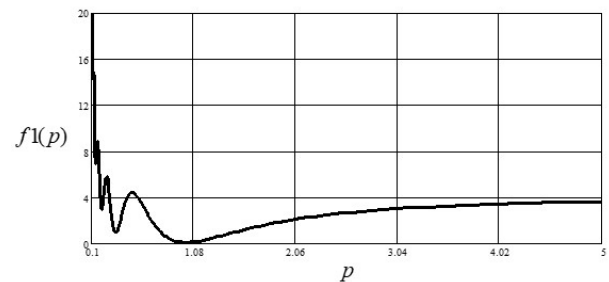

Figure 5. Graph of the function $f_1(p)$

Mode I

First, the mode described with a minus sign in front of the root in the velocity equation (44) is tested together with whether the condition (47) is met.

In the equation (44) the velocity is positive if the numerator is positive. This is obtained for the case when the term under the root is less than one, i.e. $1 - \left(1 - A^2/\Delta^2\right)\cdot\left(S_1^2 + 1\right) < 1$. From here is obtained that

$|\Delta| > A$. In the case when $\Delta > A$, the system oscillates without any impact.

Mode II

Furthermore, similarly to mode 1, the mode described with the minus sign in front of the root in the equation (44) is tested together with whether the condition (47) is satisfied.

In this case, it is tested when the term under the root in equation (44) is greater than one, i.e. $1 - (1 - A^2/\Delta^2) \cdot (S_1^2 + 1) > 1$. From here is obtained that $|\Delta| < A$. In the case when $\Delta < A$, the system oscillates with an impact.

After this, testing should be carried out when the condition (47) is met. In this case, the numerator in (44) is negative, so the denominator must be negative if the velocity is to be positive. The denominator in equation (44) is negative for $D_1 < 0$, i.e., when $p < l$.

Mode III

Finally, the mode described with the plus sign in front of the root in the velocity equation (44) is tested. Together with this, the satisfaction of the condition (47) is tested.

In this case, it is tested when the term under the root in equation (44) is greater than one, i.e. $1 - (1 - A^2/\Delta^2) \cdot (S_1^2 + 1) > 1$. And from here is obtai– ned that $|\Delta| < A$. In the case when $\Delta < A$, the system oscillates with an impact as well.

Afterwards, testing should be conducted when the condition (47) is met. In this case, the numerator in (44) is positive, so the denominator must be positive if the velocity is to be positive. The denominator in equation (44) is positive for $D_1 > 0$, i.e., when $p < l$.

Figures 6 and 7 show the areas of existence of the VI modes I, II and III. The graphs were constructed according to equation (45), where $R = 0.7$ and $\Delta_y = 0.2\pi$, when $l = 1$ (Figure 6) and $l = 3$ (Figure 7). Based on the results obtained for these three modes, it can be concluded that within frequency interval p, a VI mode of multiplicity $l=1,3,...$ can exist for all real parameter values that satisfy condition $|\Delta| < A$. When condition $\Delta = A$ is met, one of the velocity values $\dot{y}_-$ becomes zero, corresponding to an oscillator in contact with a stop, but without an impact. Under condition $\Delta > A$, the system oscillates without impact, referred to as mode I.
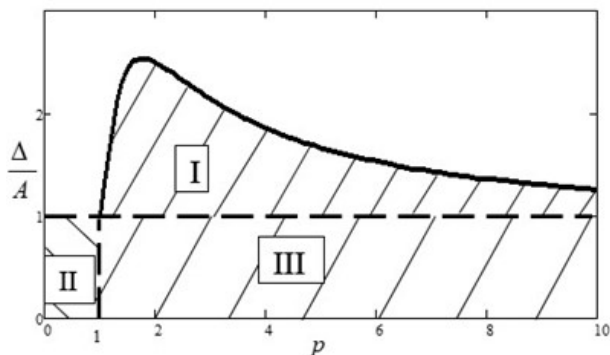

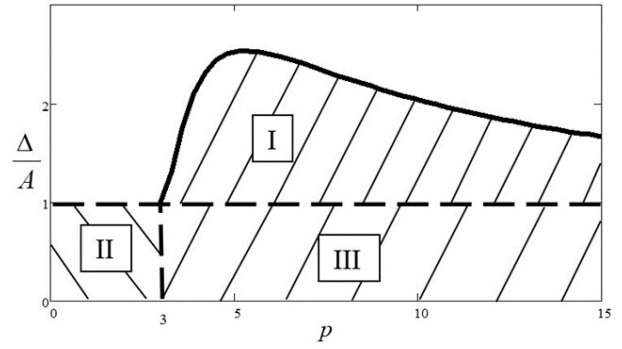Figure 6. Areas of existence of the VI modes for *l*=1

Figure 7. Areas of existence of the VI modes for *l*=3

From Figures 6 and 7, it is evident that with an increase of multiplicity l, the areas of existence of the VI also increase. The diagrams in Figures 6 and 7 make it possible to determine the frequency interval of the VI process for a known distance value Δ .

Figure 8 illustrates a phase portrait of a VI oscillator for period T, for two different values of the damping decrement, i.e. for $\Delta_y = 0.1\pi$ and $\Delta_y = 0.2\pi$ when the following data are known: $F_1 = 2N$, $Y_1 = 2N$, $m = 1kg$, $\omega_y = 1\text{s}^{-1}$, $\Delta = 1\text{m}$, $p = 1.5$, $\Omega = 1.5\text{s}^{-1}$.
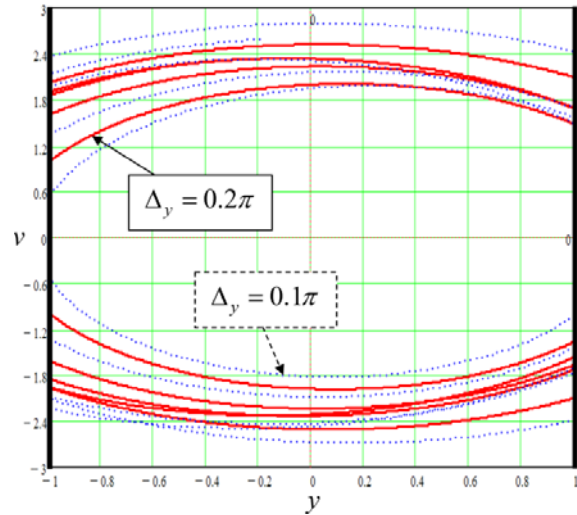

Figure 8. Phase portrait of a VI oscillator

3.2 Regions for the existence of periodic VI regimes when *l* isan even number

When l is even, i.e. $l = 2,4,...$ equations (31), (32), (36), (39) are combined into the following system:

$$\Delta = B_1 + A\cos(\psi),$$

$$\frac{-R \cdot \dot{y}_-}{\omega_y} = -\frac{\Delta_y}{2\pi} B_1 + B_2 - A \cdot p \cdot \sin(\psi),$$

$$-\Delta = e^{-\frac{\Delta_y l}{2p}} \left(B_1 \cos\left(\frac{\pi \cdot l}{p}\right) + B_2 \sin\left(\frac{\pi \cdot l}{p}\right) \right) + A\cos(\psi), \quad (48)$$

$$\frac{-\dot{y}_-}{\omega_y} = -\frac{\Delta_y}{2\pi} \cdot e^{-\frac{\Delta_y l}{2p}} \left(B_1 \cos\left(\frac{\pi \cdot l}{p}\right) + B_2 \sin\left(\frac{\pi \cdot l}{p}\right) \right) +$$

$$+ e^{-\frac{\Delta_y l}{2p}} \left(-B_1 \sin\left(\frac{\pi \cdot l}{p}\right) + B_2 \cos\left(\frac{\pi \cdot l}{p}\right) \right) - A \cdot p \cdot \sin(\psi).$$

From the system (48), the following is obtained:

$$B_1 = \Delta - A\cos(\psi), \quad B_2 = B_1 \cdot d_2 - f$$

$$d_2 = \frac{e^{\frac{\Delta_y l}{2p}} - \cos\left(\frac{\pi \cdot l}{p}\right)}{\sin\left(\frac{\pi \cdot l}{p}\right)}, \quad f = \frac{2\Delta \cdot e^{\frac{\Delta_y l}{2p}}}{\sin\left(\frac{\pi \cdot l}{p}\right)}$$

$$D_2 = \frac{(R-1)\cdot\sin\left(\frac{\pi \cdot l}{p}\right)}{2\cos\left(\frac{\pi \cdot l}{p}\right) - e^{\frac{\Delta_y l}{2p}} - e^{-\frac{\Delta_y l}{2p}}}$$

$$S_2 = \frac{1}{p}\left(\frac{R}{D_2} + \frac{e^{\frac{\Delta_y l}{2p}} - \cos\left(\frac{\pi \cdot l}{p}\right) - \frac{\Delta_y}{2\pi}\sin\left(\frac{\pi \cdot l}{p}\right)}{\sin\left(\frac{\pi \cdot l}{p}\right)}\right) \quad (49)$$

$$E = -\frac{2\cdot e^{\frac{\Delta_y l}{2p}}}{p\cdot\sin\left(\frac{\pi \cdot l}{p}\right)} - \frac{2D_2}{p}\cdot\frac{\left(e^{\frac{\Delta_y l}{2p}} - \cos\left(\frac{\pi \cdot l}{p}\right)\right)^2}{(R-1)\cdot\sin^2\left(\frac{\pi \cdot l}{p}\right)}$$

$$H = \frac{e^{\frac{\Delta_y l}{2p}} - \cos\left(\frac{\pi \cdot l}{p}\right) + \frac{\Delta_y}{2\pi}\sin\left(\frac{\pi \cdot l}{p}\right)}{(R-1)\sin\left(\frac{\pi \cdot l}{p}\right)}$$

$$\sin(\psi) = \frac{\Delta}{A}\left(D_2 \cdot S_2 \cdot \frac{\dot{y}_-}{\omega_y \cdot \Delta} + E\right),$$

$$\cos(\psi) = \frac{\Delta}{A}\left(1 - D_2 \cdot \frac{\dot{y}_-}{\omega_y \cdot \Delta} + 2\cdot D_2 \cdot H\right)$$

After several transformations in (49), the velocity equation becomes:

$$\dot{y}_- = \frac{2D_2 - 2D_2 S_2 E + 2HD_2^2}{2D_2\left(S_2^2+1\right)}\cdot\omega_y\cdot\Delta \pm$$
$$\pm\frac{\sqrt{\left(-2D_2 + 2D_2 S_2 E - 2HD_2^2\right)^2 - 4D_2^2\left(S_2^2+1\right)\left(1 - \frac{A^2}{\Delta^2} + 2HD_2 + 4D_2^2 H^2 + E^2\right)}}{2D_2\cdot\left(S_2^2+1\right)}\cdot\omega_y\cdot\Delta \quad (50)$$

The velocity equation (50) is much more complex than the velocity equation (44). Therefore, the research is more complicated when l is even ($l = 2,4,...$).

In order to estimate when the velocity is positive, the sign of D_2 is analyzed first in (49). If the numerator and the denominator have the same signs, D_2 is always positive.

Firstly, is analyzed the numerator in the equation for D_2, where the value $(R-1)$ is always negative, because $R < 1$. Sine function in the numerator is positive for $p > l$, and negative when $p < l$.

The graph of the denominator of the expression D_2, given by function $f2(p) = 2\cos\left(\frac{\pi \cdot l}{p}\right) - e^{\frac{\Delta_y l}{2p}} - e^{-\frac{\Delta_y l}{2p}}$, is shown in Figure 9. The graph was constructed for $l = 2$ and $\Delta_y = 0.2\pi$. The graph is negative for the whole interval $p \in [0,\infty]$, and shows that the denominator is negative. In the end, it can be concluded that the sign for D_2 is determined only by the sinusoidal function of the numerator.
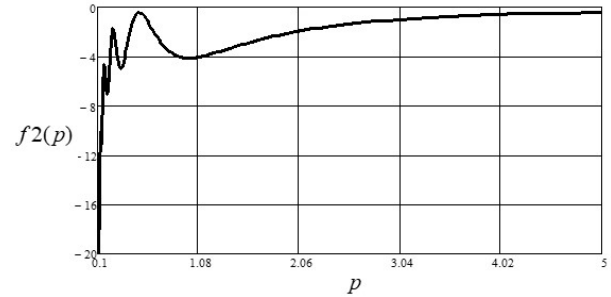

Figure 9. Graph of the function $f_2(p)$

The analysis of equation (50) determines the regions where the VI modes exist. First, it is necessary to find the region where the velocity $\dot{y}_-$ values are real. This is achieved by ensuring that the term under the square root in (50) is positive. Thus, the first condition defining the area where real velocity $\dot{y}_-$ values are located is given by:

$$\frac{|\Delta|}{A} \le \sqrt{\frac{4D_2^2\left(S_2^2+1\right)}{4D_2^2\left(S_2^2+1\right)\left(1+2D_2 H + 4D_2^2 H^2 + E^2\right)^2 - \left(-2D_2 + 2D_2 S_2 E - 2HD_2^2\right)^2}} \quad (51)$$

To find the regions of the VI, the second condition, saying that the velocity (50) is greater than zero, is introduced:

$$\dot{y}_- > 0 \quad (52)$$

The regions where VI exists are determined from the velocity equation (50) by testing when the condition (52) is met. After several transformations, equations (53) and (54) are obtained as follows.

$$\frac{|\Delta|}{A} \ge \frac{1}{\sqrt{1 + 2D_2 H + 4D_2^2 H^2 + E^2}} \quad (53)$$

Equation (53) represents the area of existence of VI for $p > l$.

$$\frac{|\Delta|}{A} < \frac{1}{\sqrt{1 + 2D_2 H + 4D_2^2 H^2 + E^2}} \quad (54)$$

Equation (54) represents the area of existence of VI for $p < l$.

Figures 10 and 11 display the regions of existence of the VI modes I and II. The graphs are constructed following equations (53) and (54), where $R = 0.7$ and $\Delta_y = 0.2\pi$, for $l = 2$ (Figure 10) and $l = 4$ (Figure 11). The solid line represents equation (53), while the dashed one represents equation (54).
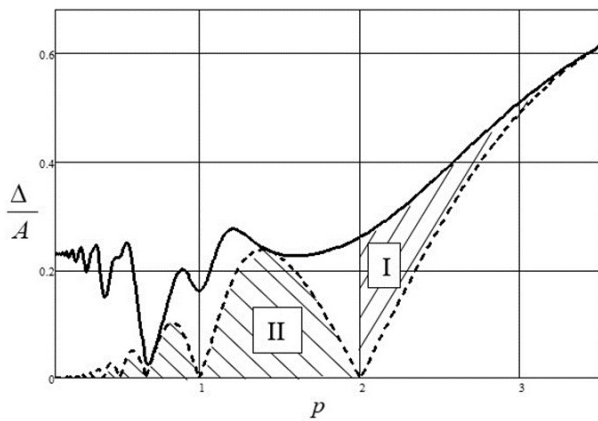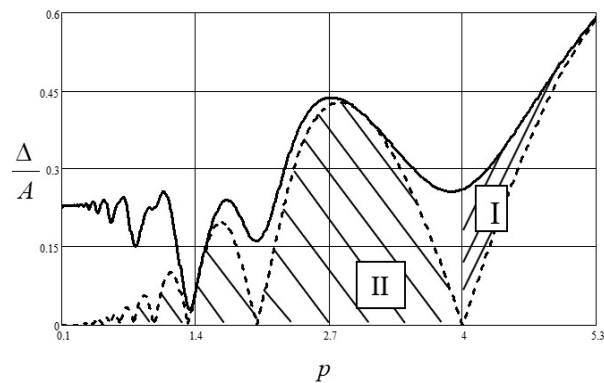
Figure 10. Regions where the VI modes exist for *l*=2

Figure 11. Regions where the VI modes exist for *l*=4

Mode I

This mode of oscillator movement corresponds to the plus sign before the square root in the equation for velocity (50). Then, the conditions $\Delta < A$ and (52) are satisfied, and the system oscillates with an impact.

Mode II

This mode of oscillator movement corresponds to the minus sign before the square root in the equation for velocity (50). Then, the condition $\Delta < A$ and (52) are met, and the system oscillates with an impact.
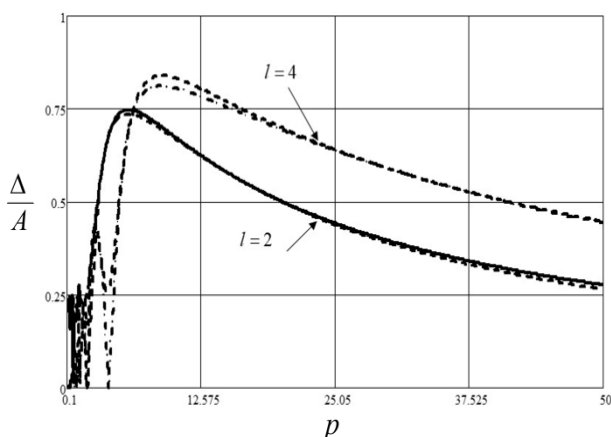

Figure 12. Areas of existence of the VI modes for *l*=2 and *l*=4

Figure 12 shows two graphs obtained for *l*=2and *l*=4 in the interval $p \in (0,50)$, where it can be seen that $\Delta < A$. This means that, when *l* is even ($l = 2,4,\ldots$),there are VI modes when $\Delta < A$, as well as there are no VI modes when $\Delta > A$.

4. ANALYSIS OF THE OBTAINED RESULTS

In this study, the VI oscillator from Figure 4 in Section 3 was analyzed. The results were obtained when *l* is odd and when*l* is even.

In Subsection 3.1, conditions (regions) where the periodic VI modes exist for definedodd values of parameter*l*. The calculation gives the equation for velocity (44), from where the regions whereVI modes exist are determined. First, the regions where the velocity values are real are determined by assuming that the term under the square root in equation (44) is positive. This leads to the first condition given in equation (45).According to condition (45), VI modes can exist within the region where the stops are positioned within the oscillation amplitude limits of the VI oscillator, specifically for $0 < \Delta < A$ (modes II and III). Additionally, they can exist outside this region for $\Delta > A$ (mode I), where oscillations occur without impacts on the stop.

To identify the regions where VI modes exist, a second condition is introduced, stating that the velocity must be greater than zero, as given in equation (47). The areas of VI existence are determined by analyzing the velocity equation (44) to see when this condition (47) is satisfied. The results are illustrated in Figures 6 and 7, which display the regions corresponding to VI modes I, II, and III.The graphs are constructed by equation (45),where $R = 0.7$ and $\Delta_y = 0.2\pi$, when $l = 1$ and $l = 3$. The figures demonstrate that as the multiplicity *l* inc–reases, the regions where the modes exist also expand.

Diagrams presented in the first part of the paper, i.e. subsection 3.1., are similar to results obtained by Babicki [1] for odd values of the mode multiplicity *l*, which shows that computation is correct and it presents validation of the results of this paper.

In Subsection 3.2 are established the conditions (or regions) where the periodic VI modes exist for even values of *l*, specifically $l = 2, 4, \ldots$. The velocity equation (50) is derived to identify these regions, and this equation is significantly more complex than the previous velocity equation (44), making the analysis more challenging when *l* is even.

Initially, the areas corresponding to real velocity values are determined by assuming the term under the square root in equation (50) is positive, which leads to the first condition described in equation (51). To further pinpoint the regions where VI modes exist, a second condition is introduced, stating that the velocity must be greater than zero, as given in equation (52). The regions of VI mode existence are then derived from the velocity equation (50) by checking when condition (52) holds. After a series of transformations applied to equation (50), the final expressions are given in equations (53) and (54). The results are illustrated in Figures 10 and 11, which depict the regions where VI modes I and II exist.The graphs are constructed by (53) and (54), where $R = 0.7$ and $\Delta_y = 0.2\pi$, when $l = 2$ (Figure 10) and $l = 4$ (Figure 11).

Based on the obtained results, it is evident that the modes for odd *l* differ from those for even *l*. The calculation shows that when *l* is odd then there are VI modes when $\Delta < A$, and vibration without impact mode

can also exist when $\Delta > A$ (Figures 6 and 7). When l is even there are VI modes when $\Delta < A$, and they do not exist when $\Delta > A$. This is shown in Figure 12 where both graphs are presented, one for $l = 2$ and another for $l = 4$ in the interval $p \in (0, 50)$, where it can be seen that $\Delta < A$.

These results, illustrated in Figures 6, 7, 10, and 11, enable the determination of the frequency interval for the realization of the VI process when the distance value is specified.

In Figure 8, a phase portrait of a VI oscillator is depicted for one period T, illustrating the behavior for two different values of the damping decrement, i.e. $\Delta_y = 0.1\pi$ and $\Delta_y = 0.2\pi$. Figure 8 shows that when there is less damping, the range of oscillations is wider.

5. CONCLUSION

This paper has presented a study of the horizontal rectilinear motion of a single-mass VI system with two symmetrical stops positioned on either side of the oscillator. The VI system, depicted in Figure 4, was modeled mathematically. The study focused on the periodic motion of the system, where the oscillator's motion period $T = 2\pi/\Omega$ is divided into two equal half-periods, $T_1 = T_2 = \pi/\Omega$. Impacts alternated between the right and left stops, occurring at constant intervals proportional to the half-period of the excitation force, $\cdot l/\Omega$, where l represents the mode multiplicity.

The research findings, which outline the conditions (or regions) wherethe periodic VI modes exist and ensure the system's stability, are illustrated in Figure 4. These results made it possible to determine the frequency interval for the VI process when the distance value Δ is known(Figures 10 and 11).

This paper presents findings for a specified form and structure of a VI system, comprising a single mass, single spring, single damper, and two stops, representing a single-degree-of-freedom VI system. These results offer insights that may assist in analyzing VI systems with varying structures, such as systems with multiple degrees of freedom, different types of external excitation forces, and more.

By analyzing the dynamic model of the VI system, it was examined what kind of relations between the parameters of the oscillator and the parameters of the coercive force can establish such periodic movements, in which the period of the impact of the oscillator on the limiter is equal to or in proportion to the period of the external force. This possibility of multiple regimes is a characteristic of VI systems, and therefore the research into the dynamics of VI systems in this paper includes the definition of all theoretically possible movements, as well as the analysis of the stability of the movement, and this allows to single out the regimes that can exist in practice.

ACKNOWLEDGMENT

REFERENCES

[1] Babicki V.I.: *Theory of Vibro-Impact Systems and Applications*, Springer-Verlag, Berlin, 1998 (Revised translation on English from Russian, Nauka, Moscow, 1978.)

[2] Garić, L.: Analysis of Vibro-Impact Processes of a Single-Mass System with Viscous Damping and a Single Limiter. Trans. of Famena, Vol. 41, No.3, pp. 29-44, 2017.

[3] Garić, L.: *The synthesis of the vibro-impact systems*, PhD thesis, University of Pristina in Kosovska Mitrovica (in Serbian), 2018.

[4] Wiercigroch, M., Kovacs, S., Zhong, S., Costa, D., Vaziri, V., Kapitaniak, M., and Pavlovskaia, E.: Versatile mass excited impact oscillator. Nonlinear Dynamics, Vol. 99, pp. 323-339, 2020.

[5] Costa, D., Vaziri, V., Kapitaniak, M., Kovacs, S., Pavlovskaia, E., Savi, M. A., and Wiercigroch, M.: Chaos in impact oscillators not in vain: Dynamics of new mass excited oscillator. Nonlinear Dynamics, Vol. 102, pp. 835-861, 2020.

[6] Sidorenko A.V. and Mavrodi A.A. Construction Machines: Lecture Course: Volume III: Machines for the Production of Building Materials, Mariupol, 2006.

[7] Wu, M.,Zhang J., and Wu H.: Vibration mitigation and energy harvesting of vibro–impact dielectric elastomer oscillators, International Journal of Mechanical Sciences, Vol. 265, pp.108906, 2024.

[8] Fan, Y., Ghayesh, M. H., Lu, T. F., and Amabili, M.: Design, development, and theoretical and experimental tests of a nonlinear energy harvester via piezoelectric arrays and motion limiters. International Journal of Non-Linear Mechanics, Vol. 142, pp. 103974, 2022

[9] Moradian, K., Raghebi, M., and Sheikholeslami, T. F.: Fabrication and Investigation of a Millimeter-Scale Electromagnetic Generator for Large-Amplitude Impact Motions, FME Transactions, Vol. 50, No. 1, 2022.

[10] Tangasawi, O., Theodossiades, S., Rahnejat, H., and Kelly, P.: Non-linear vibro-impact phenomenon belying transmission idle rattle. Proceedings of the Institution of Mechanical Engineers, Part C: Journal of Mechanical Engineering Science, Vol. 222, No.10, pp. 1909-1923, 2008.

[11] Stefani, G., De Angelis, M., and Andreaus, U.: Exploit the study of the scenarios for the control of the response of single-degree-of-freedom systems with bumpers. Journal of Sound and Vibration, Article ID 118341, 2024.

[12] Joseph, A.V. and Thampi, G.: Engine block vibrations: An indicator of knocking in the SI engine, FME Transactions, Vol. 51, No. 3, pp. 396-404, 2023.

[13] Tsai, C.P. and Li, W.C.: Micromechanical vibro-impact systems: a review. Journal of Micromechanics and Microengineering, Vol. 33, pp. 093001, 2023.

[14] Gendelman OV, Alloni A, Dynamics of forced system with vibro-impact energy sink. Journal of Sound and Vibration, Vol. 358, pp. 301-314, 2015.

[15] Xu M, Wang Y, Jin XL, Huang ZL, Yu TX, Random response of vibro-impact systems with inelastic contact. International Journal of Non-Linear Mechanics, Vol. 52, pp. 26-31, 2013.

[16] Wang J, Wang H, Wang T: External periodic force control of a single-degree-of-freedom vibro impact system. Journal of Control Science and Engineering, Article ID 570137, 2013.

[17] Perchikov N, Gendelman O.V., Dynamics and stability of a discrete breather in a harmonically excited chain with vibro-impact on-site potential. Physica D: Nonlinear Phenomena, Vol. 292, pp.8-28, 2015.

[18] Kember S.A., Babicki V.I., Excitation of vibro impact system by periodic impulses, Journal of Sound and Vibration Vol. 227, No. 2, pp. 427-447, 1999.

[19] Peterka F.: Dynamik of double impact oscillators, FactaUniversitatis: Mechanics, Automatic Control and Robotics, Vol. 2, No. 10, pp. 1177-1190, 2000.

[20] Liu Y., Pavlovskaia E., Wiercigroch M., Peng Z., Forward and backward motion control of a vibro-impact capsule system. International Journal of Non-Linear Mechanics, Vol. 70, pp. 30-46, 2015.

[21] Brindeu L., Stability of the periodic motions of the vibro-impact systems. Chaos, Solitons and Fractals Vol. 11, No. 15, pp. 2493-2503, 2000.

[22] Wang J., Shen Y., Yang S.: Dynamical analysis of a single degree-of-freedom impact oscillator with impulse excitation, Advances in Mechanical Engineering Vol. 9, No. 7, pp. 1-10, 2017.

[23] De Souza S.L.T., Caldas I.L.: Controlling chaotic orbits in mechanical systems with impacts. Chaos, Solitons and Fractals Vol. 19, No.1, pp. 171-178, 2004.

[24] Mao J., Fu Y., Li P.: Dynamics of periodic impulsive collision in escapement mechanism. Shock and Vibration, Vol. 20, Article ID 350429, 2013.

[25] Kumar, P., Narayanan, S., and Gupta, S.: Dynamics of stochastic vibro-impact oscillator with compliant contact force models. International Journal of Non-Linear Mechanics, Vol. 144, pp. 104086, 2022.

[26] Karayannis, I., Vakakis, A. F., and Georgiades, F.: Vibro-impact attachments as shock absorbers. Proceedings of the Institution of Mechanical Engineers, Part C: Journal of Mechanical Engineering Science, Vol. 222, No. 10, pp. 1899-1908, 2008.

[27] Andreaus, U., and De Angelis, M.: Influence of the characteristics of isolation and mitigation devices on the response of single-degree-of-freedom vibroimpact systems with two-sided bumpers and gaps via shaking table tests. Structural Control and Health Monitoring, Vol. 27, No. 5, e2517, 2020.

[28] Brzeski, P., Pavlovskaia, E., Kapitaniak, T., and Perlikowski, P.: Controlling multistability in coupled systems with soft impacts. International Journal of Mechanical Sciences, Vol. 127, pp. 118-129, 2017.

[29] Mélot, A., Perret-Liaudet, J., and Rigaud, E.: Vibro-impact dynamics of large-scale geared systems. Nonlinear Dynamics, Vol. 111, No. 6, pp. 4959-4976, 2023.

[30] Nešić, N., Cajić, M., Karličić, D., and Janevski, G.: Nonlinear superharmonic resonance analysis of a nonlocal beam on a fractional visco-Pasternak foundation. Proceedings of the Institution of Mechanical Engineers, Part C: Journal of Mechanical Engineering Science, Vol. 235, No. 20, pp. 4594-4611, 2021.

[31] Nešić, N., Karličić, D., Cajić, M., Simonović, J., and Adhikari, S.: Vibration suppression of a platform by a fractional type electromagnetic damper and inerter-based nonlinear energy sink, Applied Mathematical Modelling, Vol. 137, Article ID 115651, 2025.

[32] Lyu, X., Gao, Q., & Luo, G.: Dynamic characteristics of a mechanical impact oscillator with a clearance. International Journal of Mechanical Sciences, Vol. 178, Article ID 105605, 2020.

[33] Luo, G. W., Lv, X. H., and Shi, Y. Q. Vibro-impact dynamics of a two-degree-of freedom periodically-forced system with a clearance: diversity and parameter matching of periodic-impact motions. International Journal of Non-Linear Mechanics, Vol. 65, pp. 173-195, 2014.

[34] Liu, Y., & Paez Chavez, J.: Controlling multistability in a vibro-impact capsule system. Nonlinear Dynamics, Vol. 88, pp. 1289-1304, 2017.

[35] Lizunov, P., Pogorelova, O., and Postnikova, T.: Optimization of a vibro-impact damper design using MATLAB tools. Strength of Materials and Theory of Structures, Vol. 112, pp. 3-18, 2024.

[36] Legrand, M.: Introductory Tutorial on Nonlinear Modal Analysis Through an Academic Vibro-Impact Oscillator. Model Order Reduction for Design, Analysis and Control of Nonlinear Vibratory Systems. Cham: Springer Nature Switzerland, pp. 277-298, 2024.

[37] Jakovlevic, M. I.: Elementi teorii optimalnogo upravlenija periodičeskimi režimami vibroudarnih sistem: Sistemi, linejnie v promežutkah meždu soudareniami, Moskva, 2010.

[38] Beards C.E.: *Structural Vibration: Analysis and Damping*, University of London, 1996.

[39] Viba, J. A.: *Optimisation and synthesis of vibro-impact machines*, Zinatne, Riga, 1988.

[40] Boria, S., Obradovic, J., & Belingardi, G.: On de–sign optimization of a composite impact attenuator

under dynamic axial crushing, FME Transac–tions, Vol. 45, No. 3, pp. 435-440, 2017.

[41] www.dd-eng.com

[42] https://dzen.ru/a/Y9eVfyy_6zrx7FbR

[43] www.stem-techno.ru

NOMENCLATURE

F_e	elastic force of a spring (N)
c_y	spring stiffness (N/m)
F_w	viscous damping force (N)
b_y	damping coefficient (Ns/m)
m	mass (kg)
y	displacement coordinate (m)
$\dot{y}$	velocity (m/s)
$\ddot{y}$	acceleration (m/s^2)
Δ	fixed distance (m)
F, F_i	external periodic excitation force (N)
t	time (s)
T	period of oscillator movement (s)
Ω	external excitation frequency (s^{-1})
Ω_1	damped circular frequency (s^{-1})
φ	initial phase of the external force (rad)
n	viscous damping coefficient (Ns/m^2)
ω_y	angular frequency of free vibration (s^{-1})
P	normalized external force (N/kg)
y_h	homogenous part of differential eq. solution
y_p	particular part of differential equation solution
B_1, B_2	integration constants of homogenous solution
D, δ	constants
M_i, N_i	integration constants of particular solution
K_i	constant
Y_i	static elongation of the spring under the action of force F$_i$ (m)
p	dimensionless frequency
Δ_y	damping decrement
R	restitution coefficient
$\dot{y}_-$	oscillator's velocity just before an impact (m/s)
$\dot{y}_+$	oscillator's velocity just after an impact (m/s)
T_1, T_2	half periods of motion (s)
l	multiplicity of mode
A	vibration amplitude due to excitation force F$_1$ (m)
ψ	vibration phase due to excitation force F_1 (rad)

ВИБРОУДАРНИ РЕЖИМИ ПРИГУШЕНОГ ЈЕДНОМАСНОГ СИСТЕМА СА ДВА ФИКСНА ГРАНИЧНИКА

Љ. Гарић, Н. Нешић

Ова студија испитује понашање виброударног система са периодичним кретањем, на који дејствује спољашна принудна сила, а који садржи масу, опругу и амортизер, чије је праволинијско кретање ограничено са два симетрична граничника. Периодична спољашња принудна сила покреће систем, при чему је период кретања осцилатора једнак или је у сразмери са периодом спољашње принудне силе. Диференцијална једначина кретања са граничним условима, решава се аналитички и разматрају се решења. Студија анализира различите режиме понашања и укључује анализу стабилности. Резултати истраживања приказују одређивање услова (области) у којима постоје периодични виброударни режими за парне и непарне вредности вишеструкости режима. Поред тога, резултати омогућавају да се одреди фреквентни интервал за виброударни процес када је познато растојање између фиксних граничника. Истраживањем динамике виброударног система у овом раду добијени су резултати који омогућавају да се дефинишу теоретски све могуће врсте кретања, као и резултати који дефинишу области стабилности кретања, а то омогућава да се издвоје режими који могу да постоје у пракси. Резултати који су добијени у овом раду могу се применити за усавршавање постојећих и развој нових виброударних алата и машина.